Available online at www.sciencedirect.com
SCIENCE DIRECT
Journal of Photochemistry and Photobiology A: Chemistry 172 (2005) 196–206
Journal of Photochemistry and Photobiology A:Chemistry
www.elsevier.com/locate/jphotochem

Excited state intramolecular proton transfer in anionic and cationic species of 2-(2′-amino-3-pyridyl)benzimidazole

S.K. Dogra*

Department of Chemistry, Indian Institute of Technology Kanpur, Kanpur 208016, India

Received 5 July 2004; received in revised form 2 December 2004; accepted 4 December 2004
Available online 18 January 2005

Abstract

Excited state intramolecular proton transfer (ESIPT) process has been studied in the monoanionic and monocationic species of 2-(2′-amino-3-pyridyl)benzimidazole (2-A3PyBI) in aqueous and organic solvents. Dual fluorescence is observed from monocationic (aqueous and alcoholic solvents, partly from non-polar and polar aprotic ones) and monoanionic species in aqueous media. Presence of different species has been characterized with the help of absorption, fluorescence excitation and fluorescence spectroscopy, as well as, time resolved fluorimetry. The electronic structure calculations were performed on each species using semi-empirical quantum mechanical AM1 method and density functional theory B3LYP with 6-31G** basis set using Gaussian 98 program to characterize the particular ionic species. Presence of electron withdrawing pyridine =N− atom and negative charge on the benzimidazole moiety plays the vital role in increasing the rate of ESIPT process.

Keywords: 2-(2′-Amino-3′-pyridyl)benzimidazole; Absorption spectrum; Fluorescence spectrum; ESIPT; Prototropic equilibrium; Theoretical calculations

1. Introduction

Intramolecular hydrogen bonding (IHB) is known to have considerable effect on the geometric, electronic, vibrational and radiationless transitional properties of the substituted aromatic molecules [1–3]. Besides its relevance in understanding the conformation in bio-molecules [4,5], the above mentioned properties have many practical utilities worthy of considerations, e.g., dye lasers [6,7], high energy radiation detectors [8], development of UV photo-stabilizers [9], molecular energy storage devices [10], fluorescent probes [11,12], etc.

Basic requirements for ESIPT reactions to take place are: (i) IHB between the acidic centers (−NH_2, −OH groups) and the basic centers (>COOH, =N− moieties) in the ground (S_0) state [13], (ii) increase in acidic and basic character of these groups on excitation to first singlet excited (S_1) state [14], (iii) ESIPT process in S_1 state should be exothermic, i.e., energy of tautomer formed by ESIPT from enol form should be lower than that of enol form [15–18], (iv) S_1 state of enol form should be of (π, π^*) in character, because the activation barrier for the conversion of enol to tautomer is the smallest for S_1 state of (π, π^*) in nature and largest for (^{3}n, π^*) triplet state [19]. Presence of first two criteria does not guarantee that ESIPT will occur and Gillespie et al. [13,16] were the first to show the absence of large Stokes shifted tautomer emission in 1-aminoanthraquinone (1-AA) and 1,4-dihydroxyanthroquinone (1,4-DHA).

In our recent studies on ESIPT process in 2-(2′-aminophenyl)benzimidazole (2-APBI) [20,21], (Scheme 1) though we observed the presence of ESIPT reaction from the acidic −NH_2 group to benzimidazole (BI) =N− atom, fluorescence quantum yield of the tautomer band (Φ_f^T) was very small as compared to that of small Stokes shifted normal emission (Φ_f^N). Ratio (Φ_f^T/Φ_f^N) in cyclohexane is 0.42 and decreases to 0.0 with increase in the polarity and protic nature of solvents. Small Φ_f^T of tautomer could be due to smaller rate of ESIPT in S_1 state as the pK_a and pK_a* values of the deprotonation reaction of −NH_2 group are >16 and 11–12, respectively. Smith et al. [22] and our group [23–25]

* Tel.: +91 5122597163; fax: +91 5122597436.
E-mail address: skdogra@iitk.ac.in.

1010-6030/$ – see front matter © 2004 Elsevier B.V. All rights reserved.
doi:10.1016/j.jphotochem.2004.12.009

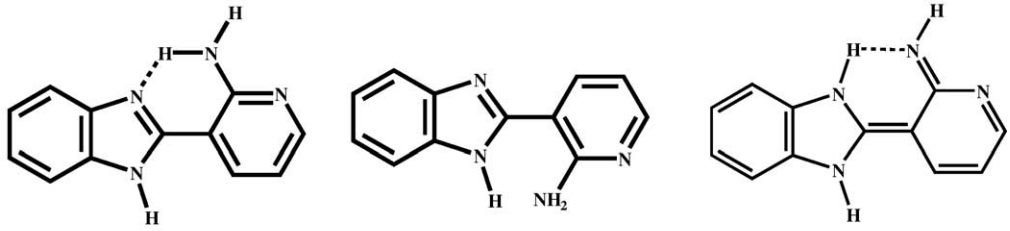

a-1 a-2 T

Scheme 1.

have shown that the rate of ESIPT process from the $-NH_2$ group can be increased either by increasing the acidity of $-NH_2$ group by replacing one of the $-NH_2$ proton by electron withdrawing group ($-COCH_3$, $-COC_6H_5$) or increasing the basicity of electron withdrawing group.

In continuation to our study on 2-APBI, we have synthesized 2-(2′-amino-3-pyridyl) benzimidazole (2-A3PyBI, Scheme 1) molecule which contain an electron withdrawing pyridine =N− atom ortho to $-NH_2$ group. Photophysics of this molecule has shown that ratio of (Φ_f^T/Φ_f^N) in 2-A3PyBI in cyclohexane increases and is much larger than that observed in 2-APBI in cyclohexane [26]. Acidity of $-NH_2$ group can be increased by protonating pyridine =N− atom or by increasing the basicity of BI moiety. Present study involves the effect of acid-base concentration on the photophysics of 2-A3PyBI, as well as, on the ESIPT reaction. Absorption, fluorescence excitation and fluorescence spectroscopy and time correlated single photon counting spectrofluorimetry has been used. Both semi-empirical (AM1) quantum mechanical and DFT-B3LYP calculations using 6-31G** as basis set, employing Gaussian 98 program were also carried out on the ionic species to supplement the experimental results.

2. Materials and methods

2-A3PyBI was synthesized by refluxing equivalent amount of 1,2-diaminobenzene and 2-aminonicotinic acid (both procured from Aldrich Chemical Company, UK) in polyphosphoric acid medium as described in literature [27]. 2-A3PyBI was purified by repeated crystallization from methanol. Purity was checked by the desired spectroscopic techniques, as well as, getting similar fluorescence and fluorescence excitation spectra using different excitation (λ_{ex}) and emission (λ_{em}) wavelengths respectively. All the solvents used were either of spectroscopic or HPLC grade from E. Merck and were used as received. Spurious emission was checked for each solvent by excitation at the same wavelength as used for each solution of 2-A3PyBI in different solvents and containing different acid-base concentrations. Triply distilled water was used for the preparation aqueous solutions.

Procedure used to prepare solutions and adjustment of pH was the same as described in our recent papers [28,29]. Hammett's acidity scale [30] was used for H_2SO_4–H_2O mixture for pH < 1 and Yagil's basicity scale [31] was used for NaOH–H_2O mixtures for pH > 13. These Hammett's and Yagil's functions represent the actual (or free) amount of protons or hydroxyl ions available in the desired solution to react with weak base or acid, respectively. Acid concentration in cyclohexane was controlled by trifluoroacetic acid (TFA), whereas in acetonitrile and methanol, it was controlled by H_2SO_4. Details of instruments used for recording absorption, fluorescence, fluorescence excitation spectra and excited state lifetimes are the same as described in our recent papers [28,29]. Fluorescence quantum yield (Φ_f) was measured from solutions having absorbance less that 0.1 using quinine sulphate in 1N H_2SO_4 as reference ($\Phi_f = 0.55$) [32]. Concentration of 2-A3PyBI was kept at 1.03×10^{-5} M to avoid self-absorption.

3. Theoretical calculations

Schemes 2–4 consider different monocations (MCs, MC-1, MC-2, MC-3 and MC2-T), dications (DCs, DC-1, DC-2 and DC-3) and monoanions (MAs, MA-1, MA-2 and MA-T), respectively for theoretical calculations. Geometry of all the species were fully optimized using AM1 method (QCMP 137, MOPAC 6/PC) [33] and using the coordinates obtained from PCMODEL [34] in S_0 and S_1 states after taking into account the configuration interactions (CI = 5 in MOPAC, 100 configurations). Total energy (E), dipole moment (μ), and dihedral angle (φ, N_8–C_9–C_{10}–C_{11}) have been compiled in Tables 1–3 for monocations, dications and monoanions, respectively. Standard single point calculations were performed on each species by taking the same geometries in S_0 and S_1 states to get the Franck–Condon absorption and fluorescence transition energies respectively. Transition energies (ΔE_{ij}) for each species were also calculated using CNDO/S-CI method [35] as described in our recent paper [28]. Total energy (E_j) was obtained by the expression ($E_j = E_i + \Delta E_{ij}$). First two transitions are compiled in the respective tables.

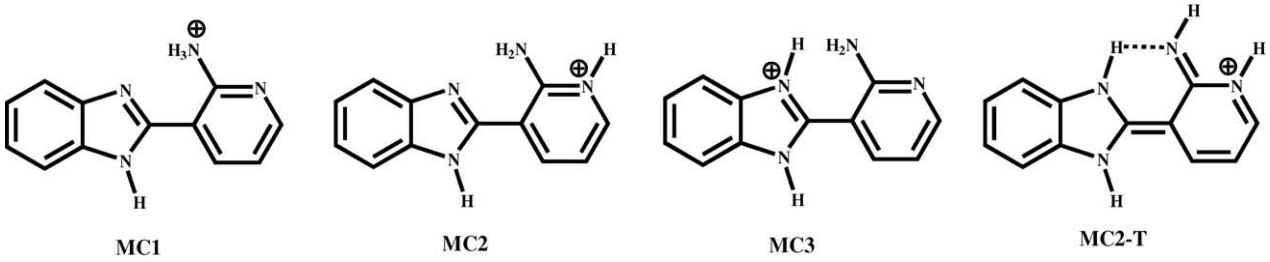

Scheme 2.

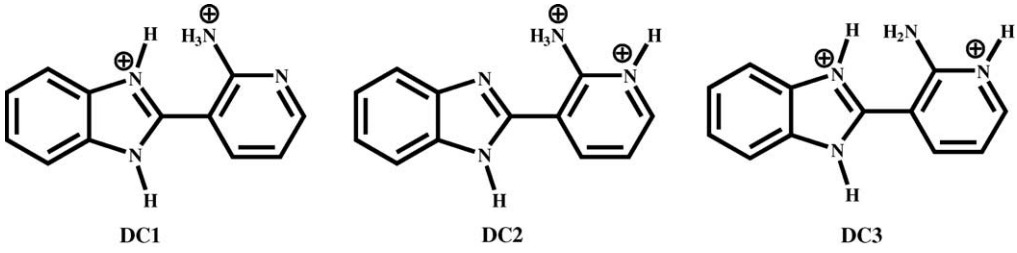

Scheme 3.

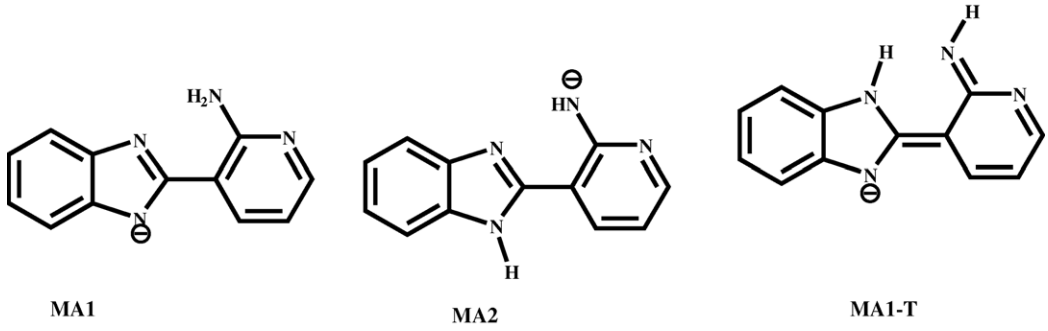

Scheme 4.

Dipolar solvation energies for different ionic species of 2-A3PyBI were calculated using the following expression based on Onsager's theory [36]

$$\Delta E_{\text{solv}} = -(\mu^2/a^3)\ f(D)$$

where $f(D) = (D-1)/(2D+1)$, D is dielectric constant of the solvent, μ is dipole moment of the fluorophore in the respective state and 'a' Onsager's cavity radius. Value of 'a' for non-spherical molecule, like 2-A3PyBI, was calculated by taking 40% of the maximum length, as suggested by Lippert [37] and it is 0.44 nm. Total energy including solvation energy for each species in water is also compiled in the respective tables.

The electronic structure calculations were carried out on each ionic species using Gaussian 98 program [38]. The geometry optimization was performed on each ionic species of 2-A3PyBI in S_0 state using DFT [39,40] B3LYP with 6-31G** basis set [38,41]. Time dependent TD [42,43] B3LYP with 6-31G** basis set was also used to calculate the excited state energies at the calculated stationary point geometry in S_0 and S_1 states. Relevant data are compiled in the respective tables.

4. Results

4.1. Absorption spectrum

Absorption spectrum of 2-A3PyBI was recorded in the acid-base concentration range of $H_0 = -10$ to $H = 16$ and relevant data have been recorded in Table 4. Absorption band maximum (λ^{ab}_{max}) at 327 nm and $H_0 = -10$ is slightly red shifted to 330 nm with slight increase in absorbance at $H_0 = -4$, suggesting slight planarity and presence of free lone pair of electrons on $-NH_2$ nitrogen atom. λ^{ab}_{max} (330, 285 nm) of the species is invariant in the range of $H_0 = -4$ to pH 0.9. Both these λ^{ab}_{max} are red shifted to 346 and 298 nm at pH 4.24, with increase in absorption and isosbestic points (λ_{isos}) at 302 and 328 nm. This suggests the presence of equilibrium between these species. With increase of pH to 8.5,

Table 1
Calculated characteristics of the probable monocations of 2-A3PyBI in the ground and excited states

Characteristics	Isomers/rotamers			
	MC1	MC2	MC3	MC2-T
AM1				
E (S_0, eV)	−2507.1110	−2507.3921	−2507.7545	−2507.3618
E (S_0, eV) (in water)	−2507.2751	−2507.8742	−2507.7770	−2507.4022
E (S_1, eV)	−2504.2575	−2504.0442	−2505.3987	−2504.8104
E (S_1, eV) (in water)	−2504.2821	−2504.0544	−2504.5504	−2504.9074
μ_g (D)	6.65	11.40	2.46	3.32
μ_e (S_1) (D)	2.57	1.65	6.39	5.15
$S_0\varphi$ (N_8-C_9-C_{10}-C_{11})(deg)	16.7	37.1	41.0	32.2
$S_1\varphi$ (N_8-C_9-C_{10}-C_{11})(deg)	15.3	33.8	64.7	16.4
CNDO/S-CI				
Transition energies (nm)				
S_0–S_1	357.3	425.3	349.3	425.9
S_0–S_2	310.7	355.7	291.4	308.0
DFT B3LYP				
Energy (Hartrees)	−682.7346	−682.8508	−682.8482	−682.7452
μ_g(D)	3.42	8.95	1.95	4.68
Transition energies (nm)				
S_0–S_1	334.6	427.4	332.9	391.9
S_0–S_2	321.2	399.7	304.6	332.2

λ^{ab}_{max} of both the band systems are blue shifted to 336 and 288 nm with decrease of absorbance. Similar to above mentioned observations, λ_{isos} are also observed at 295, 305 and 332 nm. Absorption spectrum of 2-A3PyBI is invariant in the pH range of 8–10. Long wavelength (LW) λ^{ab}_{max} is invariant to increase in pH but absorbance increases up to pH 12.9, whereas the middle wavelength (MW) and short wavelength (SW) λ^{ab}_{max} are red shifted from 288 to 298 nm and 248 to 250 nm, respectively, with λ_{isos} at 288 nm. All the λ^{ab}_{max} remain constant up to 13.5, and only LW λ^{ab}_{max} is red shifted to 339 nm, with slight increase in absorbance. Unlike the earlier behavior no clear λ_{isos} point are observed even up to H_- 16, except that change in absorbance is the minimum at 320 nm. pK_a values for the various equilibria were determined using absorption data and mentioned at the top of the arrows in Scheme 5.

Table 2
Calculated characteristics of the probable dications of 2-A3PyBI in the ground and excited states

Characteristics	Isomers/Rotamers		
	DC1	DC2	DC3
AM1			
E (S_0, eV)	−2511.0571	−2510.0984	−2511.8523
E (S_0, eV) (in water)	−2511.1979	−2510.9770	−2512.1574
E (S_1, eV)	−2508.2788	−2509.0814	−2508.9426
E (S_1, eV) (in water)	−2508.3580	−2509.1599	−2508.9841
μ_g (D)	6.17	15.47	9.10
μ_e (S_1)(D)	4.65	4.63	3.37
$S_0\varphi$ (N_8-C_9-C_{10}-C_{11})(deg)	88.3	0.0	88.7
$S_1\varphi$(N_8-C_9-C_{10}-C_{11})(deg)	88.1	0.1	88.7
CNDO/S-CI			
Transition energies (nm)			
S_0–S_1	336.4	523.4	336.6
S_0–S_2	320.2	435.4	322.6
DFT B3LYP			
Energy (Hartrees)	−682.9663	−683.0047	−683.0039
μ_g (D)	6.17	8.63	8.63
Transition energies (nm)			
S_0–S_1	307.6	391.0	307.6
S_0–S_2	290.8	368.9	290.8

Table 3
Calculated characteristics of the probable monoanions of 2-A3PyBI in the ground and excited states

Characteristics	Isomers/rotamers		
	MA1	MA2	MA1-T
AM1			
E (S_0, eV)	−2487.7211	−2486.9925	−2487.4339
E (S_0, eV) (in water)	−2487.7521	−2487.3636	−2487.5188
E (S_1, eV)	−2484.8034	−2484.7409	−2484.9693
E (S_1, eV) (in water)	−2484.8098	−2484.8598	−2484.9700
μ_g(D)	2.86	9.93	4.77
μ_e (S_1) (D)	1.30	5.61	0.43
$S_0\varphi$(N_8-C_9-C_{10}-C_{11})(deg)	0.0	36.0	0.0
$S_1\varphi$(N_8-C_9-C_{10}-C_{11})(deg)	0.0	35.2	0.5
CNDO/S-CI			
Transition energies (nm)			
S_0–S_1	359.5	431.1	417.7
S_0–S_2	321.6	327.7	320.2
DFT B3LYP			
Energy (Hartrees)	−681.8024	−681.7550	−681.7884
μ_g (D)	1.49	10.01	3.32
Transition energies (nm)			
S_0–S_1	341.2	467.0	408.6
S_0–S_2	320.9	364.3	314.9

Table 4
Absorption band maxima (λ^{ab}_{max}, nm), fluorescence band maxima (λ^{f}_{max}, nm), fluorescence quantum yield (Φ_f) and excited state lifetimes (τ, ns) of different ionic species of 2-A3PyBI

Species/solvents	λ^{ab}_{max}	λ^{f}_{max} (Φ_f)	τ_1^N	τ_2^N	τ_1^T
Water (N) pH = 8.5	248, 288, 336	404, 534 (0.0958)(0.0698)	0.52 (26)	2.64 (74)	
				2.52 (13.2)	1.33 (86.5)
Water monocation pH = 4.24	298, 346	434, 502 (0.0415)(0.1188)	0.78 (85.5)	4.6 (14.5)	
				4.4 (5.5)	1.21 (94.2)
Water dication $H_0 = -4$	285, 330	422 (0.4199)	2.50		
Water trication $H_0 = -10$	287, 327	423 (0.3610)	–	–	–
Water monoanion pH = 12.6	250, 298, 336	409, 515 (0.0229)(0.1024)	2.84 (18.6)	4.31 (81.4)	
				4.46 (48.3)	2.34 (51.7)
Water dianion H_- = 15.9	285, 339	501 (0.3312)	–	–	–
Cyclohexane + TFA = 0 M	284, 294, 350, 363 (sh)	379, 392, 550, 577			
Cyclohexane + TFA = 10^{-3} M	288, 345, 358	405, 435, 508			
Cyclohexane + TFA = 0.1 M	288, 330	425			
Acetonitrile + 0 M H_2SO_4	285, 293, 345, 357	397, 417, 542, 578			
Acetonitrile + 10^{-5} M H_2SO_4	298, 352	428, 505			
Acetonitrile + 1 M H_2SO_4	285, 330	425			
Methanol + 0 M H_2SO_4	286, 294, 346, 360	402, 539			
Methanol + 10^{-4} M H_2SO_4	300, 355	432, 515, 535			
Methanol + 1 M H_2SO_4	285, 332	428, 506, 541			

4.2. Fluorescence spectrum

Fluorescence spectral characteristics of different ionic species of 2-A3PyBI in the H_0/pH/H range of –10 to 16 are compiled in Table 4. At pH 8.5, neutral species of 2-A3PyBI possesses a dual fluorescence with fluorescence band maximum (λ^{f}_{max}) at 404 and 534 nm. Ratio of I_f (534)/I_f (404) is 0.73 and remains unchanged in the pH range of 7.8–9.8. With increase of basic strength, dual emission is retained. SW λ^{f}_{max} band is red shifted to 409 nm with decrease of fluorescence intensity and LW λ^{f}_{max} is blue shifted to 515 nm with increase of fluorescence intensity with ratio (I_f (515)/I_f (409) increases to 0.47. Isoemissive points are observed at 467 and 540 nm in pH range of 8.0–12.6 as depicted in Fig. 1. In the range of pH 12.6 to H_- 15.9, dual emission is changed in to a single fluorescence band at 501 nm with large increase of fluorescence intensity and its saturation is not complete even at H_- = 15.9. This is depicted by the presence of weak emission at 409 nm and highest base strength used, as shown in Fig. 2.

On the other hand, emission characteristics of 2-A3PyBI are more complex than the absorption spectrum with increase in acid strength. In the pH range 8.5–4.24, similar to neutral species, dual emission is observed with the difference that SW 404 nm emission band is red shifted to 434 nm and LW 534 nm one is blue shifted to 502 nm. Ratio I_f (502)/I_f (434) increases to 2.81 from 0.6 for neutral species. Isoemissive points are observed at 414 and 541 nm as shown in Fig. 3.

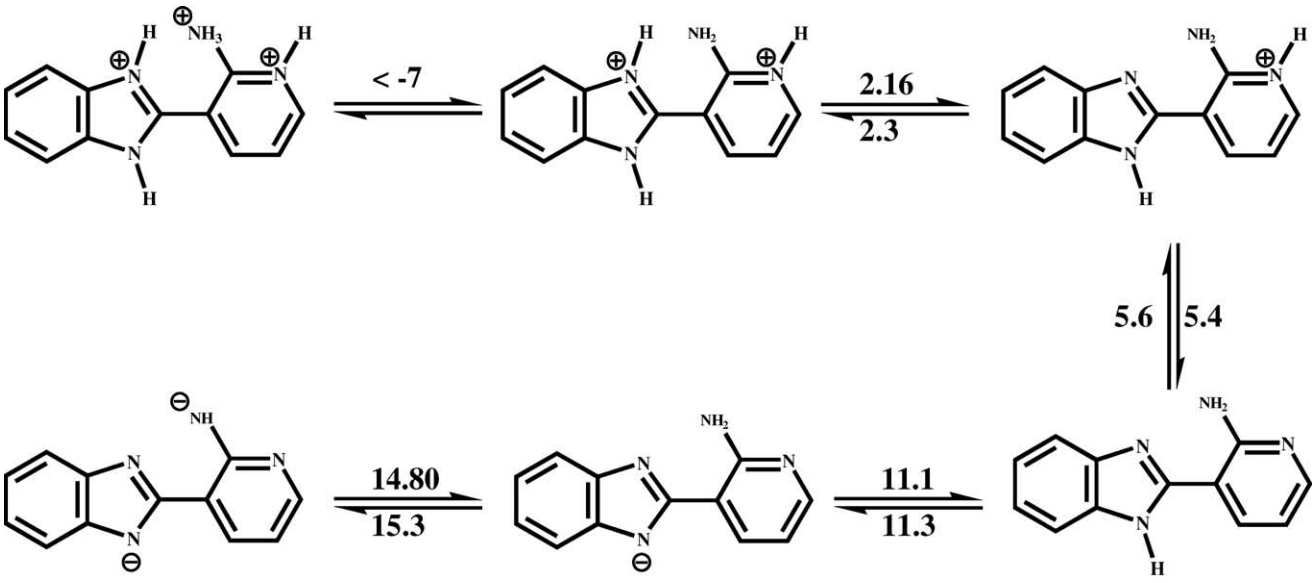

Scheme 5.

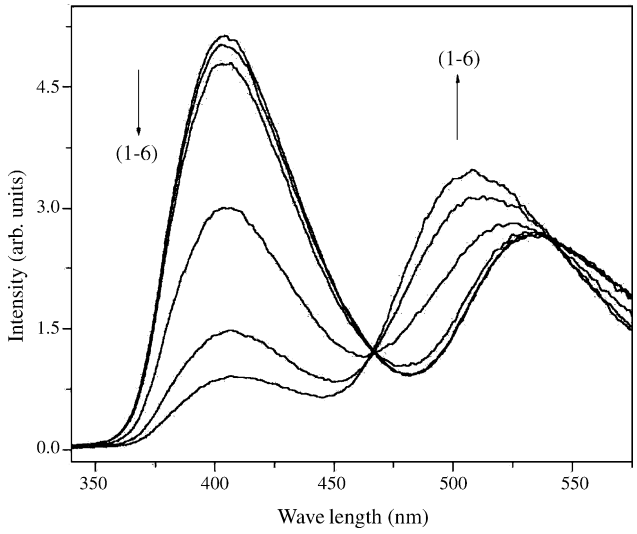

Fig. 1. Fluorescence spectrum of 2-A3PyBI in the pH range of 8.1–12.9. 1, 8.5; 2, 9.3; 3, 10.5; 4, 11.3; 5, 11.9; 6, 12.9. λ_{exc} = 290 nm. [2-A3PyBI] = 1.03×10^{-5} M.

Fig. 3. Fluorescence spectrum of 2-A3PyBI in the pH range of 4–8.5. (1) pH 4.0; (2) pH 5.0; (3) pH 5.7; (4) pH 6.1; (5) pH 7.1; (6) pH 8.5. λ_{exc} = 340 nm. [2-A3PyBI] = 0.5×10^{-5} M.

Fig. 4 depicts the emission spectra of 2-A3-PyBI in the pH range of 4.24 to 0.9. Dual emission is still observed but 502 and 434 nm bands shift to 522 and 422 nm respectively. Decrease in the fluorescence intensity of SW emission is more than that in LW emission such that I_f (522)/I_f (422) increases to 1.22. With further increase of acid strength, dual emission converts to single emission with λ^{f}_{max} at 423 nm, with increase in fluorescence intensity (Fig. 5). This behavior is different from that observed in the absorption spectrum as no changes are observed in λ^{ab}_{max} and absorbance during this range of acid concentration. Fluorescence intensity keeps on decreasing with out any change in λ^{f}_{max} with acid concentration up to $H_0 = -10$.

Effect of λ_{ex} in the range of 300–360 nm was studied at $H_0 = -10$, -4 and 0.0; pH 4.2, 7.8, 9.8 and 12.6 and H_- 16. Fluorescence band maxima of dual emission and their fluorescence quantum yields are invariant, suggesting that emission is occurring from their most relaxed states.

4.3. Fluorescence excitation spectrum

In order to assign the nature of emitting species in the H_0/pH/H_- range of –10 to 16, fluorescence excitation spectra were recorded at H_0 –10, -3 and 0, pH 4.2, 8.5 and 12.0 and H_- 16 and in the emission wavelength (λ_{em}) range of 400–570 nm. At H_0 –10 and –3 and H_- 16, the fluorescence excitation spectra recorded at all the emission wavelengths

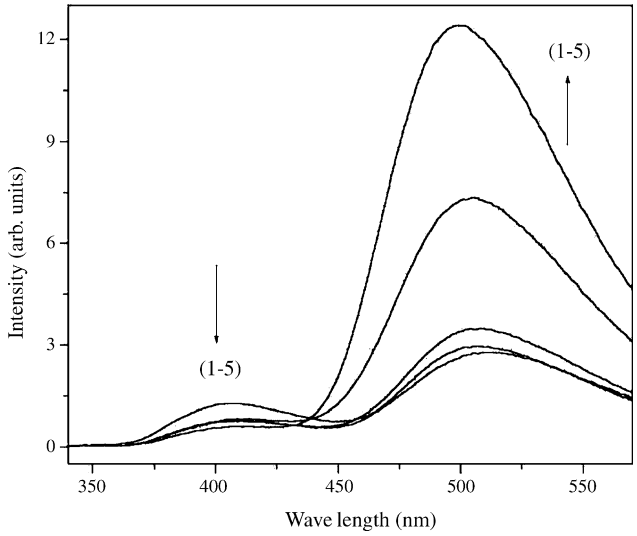

Fig. 2. Fluorescence spectrum of 2-A3PyBI at different basic concentration. (1) pH 12; (2) pH 13; (3) pH 14.0; (4) H_- 15.0; (5) H_- 15.9. λ_{exc} = 290 nm. [2-A3PyBI] = 0.5×10^{-5} M.

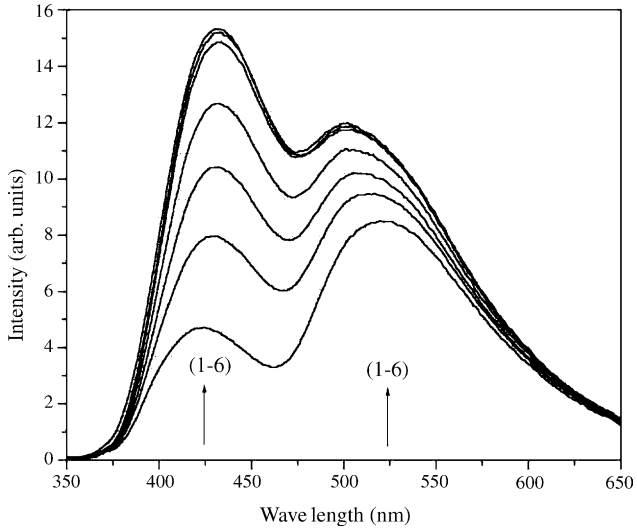

Fig. 4. Fluorescence spectrum of 2-A3PyBI in the pH range of 0.89 to 4.24. (1) pH 0.89; (2) pH 2.23; (3) pH 2.4; (4) pH 2.76; (5) pH 3.17; (6) pH 4.24. λ_{exc} = 328 nm. [2-A3PyBI] = 1.67×10^{-5} M.

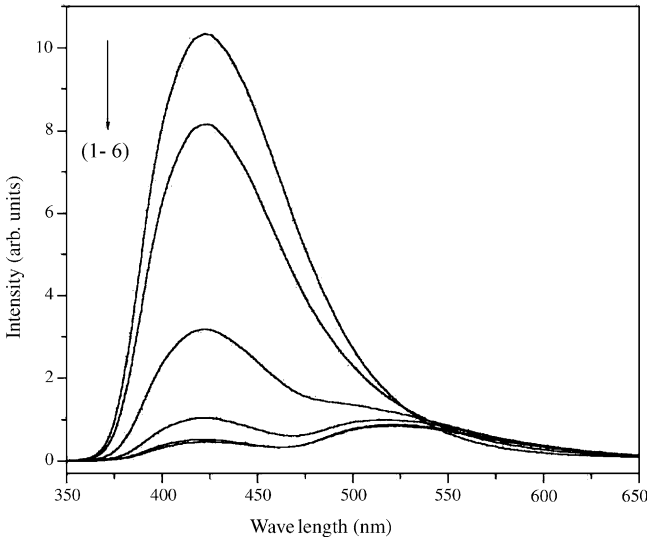

Fig. 5. Fluorescence spectrum of 2-A3PyBI at different acid concentrations. (1) H_0 –3.8; (2) H_0 –2.90; (3) H_0 –1.84; (4) H_0 –0.90; (5) pH 0.04; (6) pH 0.89. λ_{exc} = 328 nm. [2-A3PyBI] = 1.67×10^{-5} M.

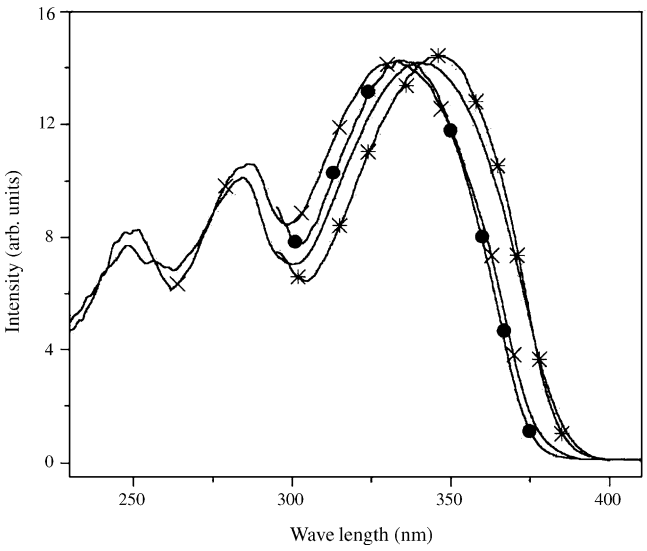

Fig. 6. Fluorescence excitation spectrum of 2-A3PyBI at some selected pH. (a) pH 4.1, (—); λ_{em} = 400 nm; (*-*-*), λ_{em} = 560 nm. (b) pH 12, (×-×-×) λ_{em} = 390 nm, λ_{em} = 360 nm, (●-●-●). [2-A3PyBI] = 1.03×10^{-5} M.

resemble with each other, as well as, with the absorption spectra at these acid-base concentrations. This clearly suggests the presence of only one species in S_0 and S_1 states and these are emitting from the most relaxed S_1 state. At all other acid-base concentrations mentioned above, fluorescence excitation spectra recorded at $\lambda_{em} < 450$ nm are blue shifted in comparison to that recorded at $\lambda_{em} > 450$ nm. This clearly suggests the presence of two species in S_0 state, resembling with the behavior that is generally observed for many neutral molecules showing ESIPT behavior [29,44–46]. Non-resemblance of the absorption spectra at these acid-base concentrations with the fluorescence excitation spectra is due to the fact that the absorption spectrum is composite absorption spectra of two species present in the system. Fig. 6 depicts the fluorescence excitation spectra of the ionic species at pH 12.0 and 4.2 at λ_{em} 400 and 560 nm.

4.4. Acid–base equilibrium in non-aqueous solvents

Absorption, fluorescence excitation and fluorescence spectra of 2-A3PyBI were also studied in cyclohexane + trifluoroacetic acid (TFA, up to 0.1 M), acetonitrile and methanol containing H_2SO_4 up to 1 M concentration. In broad sense the absorption spectra of all the species so formed at different acid concentration are similar to that observed in aqueous medium. In cyclohexane containing TFA up to 10^{-4} M concentration, SW small Stokes shifted emission is the main band (405, 429 nm) with a small shoulder at 508 nm. With increase of TFA concentration, a new band appears at 425 nm at 10^{-2} M. With increase in polarity of solvents, i.e., in acetonitrile + 10^{-5} M H_2SO_4, the fluorescence intensity of 508 nm band is greater than that observed in cyclohexane +10^{-3} M TFA and this further increases in methanol +10^{-4} M H_2SO_4. At H_2SO_4 concentration >10^{-2} M, only one emission band is observed at 425 and 428 nm in acetonitrile and methanol respectively. Presence of tautomer emission at ∼ 506 nm in methanol containing 1 M H_2SO_4, suggests that (similar to that in aqueous medium) DC has not been completely formed. Behavior of fluorescence excitation spectrum at each acid concentration in the respective solvent is similar to their absorption spectrum in these solvents and similar to that observed in aqueous medium. Figs. 7–9 depict the fluorescence spectra of 2-A3PyBI at different acid concentration in cyclohexane, acetonitrile and methanol, respectively.

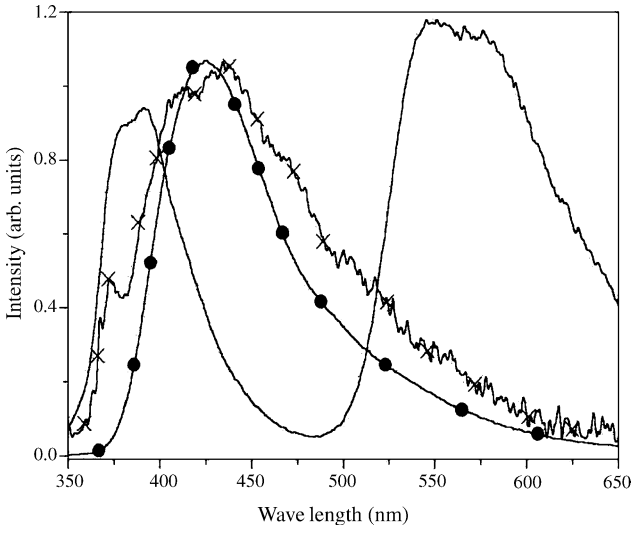

Fig. 7. Fluorescence spectrum of 2-A3PyBI in cyclohexane containing different amount of TFA. (—), 0 M TFA; (×-×-×), 10^{-5} M TFA; (●-●-●), 0.1 M TFA, [2-A3PyBI] = 0.5×10^{-5} M. λ_{exc} = 350 nm.

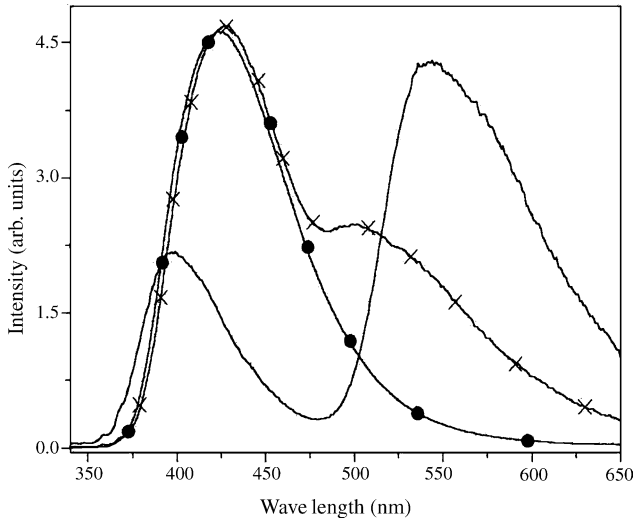

Fig. 8. Fluorescence spectrum of 2-A3PyBI in acetonitrile containing different amount of H_2SO_4. (—), 0 M H_2SO_4; (×-×-×), 10^{-5} M H_2SO_4; (•-•-•), 0.1 M H_2SO_4. [2-A3PyBI] = 0.5×10^{-5} M. λ_{exc} = 330 nm.

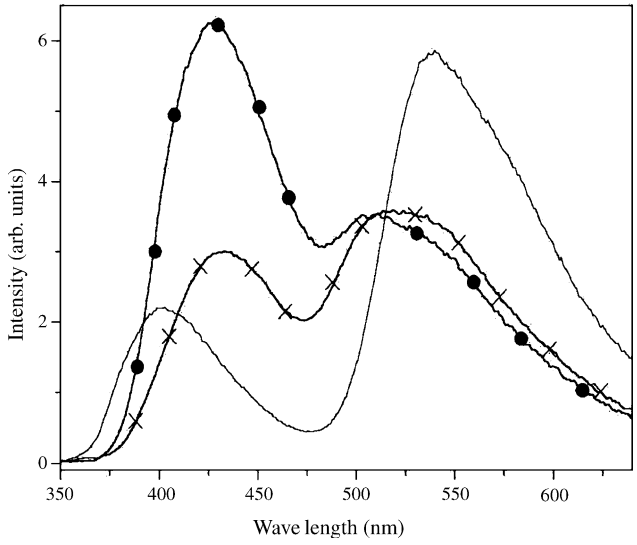

Fig. 9. Fluorescence spectrum of 2-A3PyBI in methanol containing different amount of H_2SO_4. (—), 0 M H_2SO_4, (×-×-×), 10^{-5} M H_2SO_4; (•-•-•), 1 M H_2SO_4. [2-A3PyBI] = 0.5×10^{-5} M. λ_{exc} = 330 nm.

5. Discussion

2-A3PyBI possesses three basic centers (pyridine =N–, BI =N– and $–NH_2$ group) and two acidic centers (>N–H and $–NH_2$ moieties). Thus this molecule can form in total six ionic/neutral species. Since there can be more than one possible ionic species, their formation and assignment will be discussed separately, followed by different prototropic equilibria.

5.1. Neutral species

It has been established [26] that 2-A3PyBI can be present as a-1 and a-2 rotamers in S_0 state (Scheme 1). λ_{max}^{ab} at 346–350 and 360–363 nm of the LW absorption spectrum belongs to a-2 and a-1, respectively in non-polar and polar-aprotic solvents. Rotamer a-3 (solvated open, not shown) will be present in water at λ_{max}^{ab} 336 nm. SW normal Stokes shifted emission (404 nm) is due to rotamer a-2 and a-3 in the above-mentioned solvents and LW large Stokes shifted (534 nm) fluorescence is due to tautomer, formed by ESIPT from a-1 in S_1 state.

5.2. Monocations

Three possible MCs can be obtained by protonating either of the basic centers (MC1, MC2 and MC3, Scheme 2) and one tautomer of MC (MC2-T, Scheme 2) formed by ESIPT in MC2. MC1 and MC2-T can be neglected in S_0 state, as these species are unstable with respect to MC3 by 62.1 and 37.9 kJ mol^{-1}, respectively under isolated conditions and 57.8 and 45.6 kJ mol^{-1}, respectively with respect to MC2 when dipolar solvation energies are included. Further activation barrier for intramolecular proton transfer in MC2 to yield MC2-T is 65.7 kJ mol^{-1} in S_0 state. Similar conclusions are also arrived at from the results of DFT B3LYP with 6-31G** basis set calculations except numbers. Under isolated conditions and using AM1 method, MC3 is stable than MC2 by 35 kJ mol^{-1}, whereas when dipolar solvation energy is included, MC2 becomes more stable than MC3 by 9.4 kJ mol^{-1}. This is because μ_g of MC2 (11.40 D) is larger than that of MC3 (2.5 D). On the other hand, DFT B3LYP theory with 6-31G** basis set predicts that MC2 is more stable than MC3 by 6.8 kJ mol^{-1}. Charge density data predict that pyridine =N– atom in both the rotamers a-1 (5.2111) and a-2 (5.1969) are more basic in comparison to BI =N- moiety in these neutral rotamers (5.1563 in a-1 and 5.1320 in a-2). Further potential energy mapping program [47] suggests that BI =N- atom is more reactive (110 kJ mol^{-1} in a-1 and 114.6 kJ mol^{-1} in a-2) than that of pyridine =N– atom (79.6 kJ mol^{-1} in a-1 and 100.3 kJ mol^{-1} in a-2) under isolated conditions. Absorption spectral data also cannot predict the formation of specific MC because protonation of pyridine =N– in 2-AP [48] and BI =N– in 2-APBI [20] leads to a red shift of the neutral spectrum by 10 nm and 13 nm, respectively, whereas in 2-A3PyBI, red shift in λ_{max}^{ab} is also 10 nm. All these data predict that MC3 is more stable than MC2 in non-polar solvents and MC2 is more stable, in polar solvents and may further be stabilized if hydrogen bonding energies of the protic solvents are added. These results can be substantiated from the following experimental data.

It is well established that ESIPT process can be observed in MC having structure MC2 and absent in MC having structure MC3 or open MC2 solvated structure. Failure of ESIPT in MC3 is confirmed from the results of prototropic reactions of 2-APBI [20], i.e., only one small Stoked shifted normal fluorescence is observed in MC of 2-APBI. In non-polar (cyclohexane) solvent, dual fluorescence is observed without TFA and $\Phi_f^T > \Phi_f^N$ [26]. As the concentration of TFA increases, fluorescence band develops at ~435 nm at the expense of 392

and 550 nm bands. A small shoulder is present at 508 nm. At TFA concentration $>10^{-4}$ M, a new small blue shifted band appears at 425 nm, having maximum intensity at 0.1 M TFA corresponding to DC (see later). This supports the above results that less polar MC3 will be favorable in non-polar solvents (cyclohexane). Shoulder at ∼508 nm only suggests the presence of small amounts of MC2 and this may be due to the polar nature of cyclohexane medium in presence of small amount of TFA (Fig. 7). As the polarity of solvents increases, e.g., acetonitrile, the intensity of the shoulder at ∼505 nm increases (Fig. 8) and behavior of the emission spectrum of 2-A3PyBI in methanol as a function of H_2SO_4 concentration (Fig. 9) is similar to that observed in aqueous medium. This is further supported by AM1 calculations in S_1 state and taking into account the configuration interactions that MC3 is the most stable followed by MC2-T suggesting that ESIPT is an exothermic process in MC2 and thus a feasible process. Potential energy mapping data also supports that reactivity to protonation of BI =N– increases from 114.6 kJ mol^{-1} to 147.0 kJ mol^{-1} on excitation to S_1 state. Smaller Φ_f^T of MC2-T than Φ_f^N of MC3 is due to smaller proportion of MC2 in the solution. Transition energies predicted by all the methods for MC3 agree nicely with experimental results.

Thus in the end it may concluded that, both MC2 and MC3 will be present in the system in the pH range of 4.24–8.5 and their proportion will depend upon the solvent polarity. Absorption and fluorescence excitation spectra of MC2 and MC3 are similar but MC3 gives rise to SW normal emission and MC2 gives rise to tautomer emission obtained by ESIPT. Lifetime measurements also suggest that SW normal emission is due to two MCs. Shorter lifetimes (0.78 ns) and longer lifetime (4.5 ns) can be assigned to the blue side and red side of the SW emission band respectively because the amplitude of the latter species decreases with increase of λ_{em}. Different lifetimes for the SW and LW emissions suggest that equilibrium is not established in S_1 state between MC2 and MC3. Only one pK_a values observed for MC-N equilibrium suggest that both the MC2 and MC3 will be formed simultaneously and confirmed by the presence of isosbestic and isoemssive points. Similar behavior is also observed in 2-(2′-mehtoxyphenyl)-3-H-imidazo[4,5-b]pyridine [49].

5.3. Dications

Scheme 3 depicts three possible DCs (DC1, DC2 and DC3). AM1 calculations support the presence of only one DC3, because DC1 and DC2 are unstable by 76.7 and 169.2 kJ mol^{-1} respectively as compared to DC3 in S_0 state under isolated conditions and by 92.6 and 113.9 kJ mol^{-1} when dipolar solvation energy is included. In case of DFT B3LYP calculations, structure of DC2 always reverts back to DC3 whenever optimized and DC1 is 100.8 kJ mol^{-1} unstable in comparison to DC3. High instability of DC2 and DC1 is due to the presence of positive charges adjacently. Blue shifts observed in the absorption and fluorescence spectra suggest the protonation of $–NH_2$ group, but this can be rejected because the protonation constant of the MC of 2-AP is –7.8 [48]. In other words, very high acid concentration is required to form DC2. Similarly the protonation constant of the MC of 2-APBI leading to similar structure as DC2 is 0.4 [20]. Whereas in the present case, pK_a value is 2.2 (see later). Above assignment of DC3 can be further supported by a single fluorescence band (Fig. 5), similar fluorescence excitation spectra monitored at different λ_{em}, resemblance of the absorption spectra with fluorescence excitation and fluorescence decay profile following single exponential (τ = 2.5 ns). Similar observations in different non-aqueous solvents support the above assignment. Blue shifts observed in the spectral characteristics are due to loss of planarity of aminopyridine ring and BI moiety, supported by dihedral angle of 88.9° (Table 2). Presence of LW emission band at 506 nm at 1 M H_2SO_4 in methanol suggests that like aqueous medium complete conversion of MC1 to DC3 is not complete at 1 M H_2SO_4.

There can be only one trication (TC), formed by protonating all the three basic centers and its presence can be detected only at $H_0 < -7.8$, as mentioned above. This is because the protonation constant for the MC of 2-AP is –7.8 [48]. Since Ar–NH_3^+ ion becomes stronger acid in S_1 state [50], no fluorescence was detected even at H_0 –10 in 2-AP. Similar behavior is also observed in 2-A3PyBI. Thus confirms its formation in S_0 state and absence in S_1 state. Similar behavior is observed in the protonation of aromatic amines, i.e. proton induced fluorescence quenching is observed before the protonation of $–NH_2$ group of aromatic amines in S_1 state [50].

5.4. Monoanions

Two possible MA's and one MA tautomer (MA1, MA2, MA1-T, Scheme 4) can be obtained by deprotonating >N–H and $–NH_2$ protons and tautomer formed by ESIPT in MA1. Results of Table 3 suggest that using AM1 calculations presence of MA2 and MA1-T can be neglected because these are unstable as compared to MA1 by 70.3 and 27.7 kJ mol^{-1} under isolated conditions and by 37.5 and 22.5 kJ mol^{-1} when dipolar solvation energies are included. In other words only one monoanion (MA1) is present in the system. This can be supplemented by the following observations. (i) Under isolated conditions, DFT (B3LYP) calculations also predict that MA2 and MA1-T are unstable by 125.5 and 36.8 kJ mol^{-1}, respectively. (ii) Agreement between the transition energies predicted by CNDO/S-CI and TD (DFT) and experimental observations is best for MA1 (Table 3). (iii) pK_a value for the deprotonation of >N–H moiety of benzimidazole in 2-APBI is 12.9 [20] and that of $–NH_2$ group in 2-aminopyridine (2-AP) [48] is >14. (iv) Activation barrier for the proton transfer in MA1 to yield MA1-T is 80.8 kJ mol^{-1}in S_0 state. Thus formation of MA1-T is not viable at room temperature in S_0 state. (v) Fluorescence band maximum of MA formed by the deprotonation of $–NH_2$ group of 2-AP is blue shifted by 12 nm whereas that of the 2-APBI was red shifted by 88 nm.

This suggests that normal small Stokes shifted emission was observed from the MA of 2-AP, whereas large Stokes shifted emission was observed from the tautomer formed by ESIPT in the MA of 2-APBI. Whereas in case of 2-A3PyBI, both normal and tautomer emission is noticed.

Having established that MA1 is the only monoanion present in the system at pH 12.9, other spectral characteristics can be explained as follows. Not much change observed in the LW λ_{max}^{ab} in the MA of 2-A3PyBI as compared to the neutral species could be due to the presence of stronger interactions between the amino pyridine ring and benzimidazolyl group in both neutral and MA. Similar behavior is also nearly observed in 2-HPBI [44] and 2-APBI [20]. Dual fluorescence observed in case of MA suggests the presence of two species in S_1 state. Fluorescence excitation spectra recorded at SW (in the range of 390–430 nm) and LW (560 nm) emission bands are slightly different, i.e., in former case λ_{max}^{ex} is at 340 nm and in latter case it is at 335 nm. Since ESIPT process can only occur in the closed form, possessing IHB (MA1) in S_0 state, large Stokes shifted LW emission band is assigned to the tautomer (MA1-T) formed from MA1 by ESIPT, possessing λ_{max}^{ex} at 335 nm. On the other hand small Stokes shifted SW normal emission is due to the solvated open MA structure (MA-3), having the λ_{max}^{ex} at 340 nm. An absence of rise time in tautomer emission (MA1-T) (not possible in our nano-second spectrofluorimeter) indicates that ESIPT in the monoanionic species is also an ultra fast process as observed in case of neutral species. Larger value of Φ_f^T ($\Phi_f^T/\Phi_f^N = 4.47$) in MA as compared to neutral species ($\Phi_f^T/\Phi_f^N = 0.73$) suggests that increase in the electron withdrawing nature of the proton accepting group increases the rate of proton transfer. This is supported by the fact that MA1-T in S_1 state, after taking in to account the configuration interactions and optimizing the geometry, is more stable than MA1 by 16 kJ mol^{-1} under isolated conditions and 15.5 kJ mol^{-1} when dipolar solvation energy is included. The activation barrier for the transformation of MA1 to MA1-T in S_1 state reduces to 65 kJ mol^{-1} from 80 kJ mol^{-1} in S_0 state. Although the activation barrier is still quite large in S_1 state, but decrease in the activation barrier suggests that ESIPT process is more favorable in S_1 state. Similar behavior has also been observed in the MA's of 2-APBI [21] and 2-AMPBI [25] species. Biexponential decay observed at both the emission wavelengths (409 and 515 nm) suggests the interference of one in to another. Shorter lifetime (2.6 ns) can be assigned to tautomer emission and longer lifetime (4.5 ns) to the open structure MA. This is because the proportion of shorter lifetime species increases with increase of λ_{em}. Further two different lifetimes suggest that the equilibrium between MA1 and MA-open structure is not established in the S_1 state.

5.5. Dianion

There can be only one DA, formed by further deprotonation of the amino group proton (Scheme 5). Small amount of fluorescence intensity observed at the SW side (~410 nm) of the main band of DA is due to MA-3 remaining in the solution even at H_- = 15.9. This is because of incomplete deprotonation of MA. This is supported by the fact that the fluorescence excitation spectrum of the solution at H_- = 15.9 monitored at SW emission resemble with that of MA-2. Presence of only one kind of DA is further supported by the single fluorescence band, similar fluorescence excitation spectra monitored at different λ_{em} of the LW emission and resemblance with absorption spectrum, fluorescence decay profile following a single exponential decay at different λ_{em} and presence of isoemissive point at ~450 nm. Invariance of λ_{max}^{f} and Φ_f of DA at different λ_{ex} (290–360 nm) also confirm the presence of single DA species. In general deprotonation of amino group of aromatic amines leads to non-fluorescent MA [50] with few exceptions [51]. But wherever the MA is fluorescent, it is large red shifted. Thus red shift observed in the absorption and fluorescence spectra of DA in comparison to the MA is consistent with the deprotonation of amino proton. Small blue shift in DA emission in comparison to the tautomer emission (MA-T) is because of the structural difference between the two ionic species.

5.6. Prototropic equilibria

pK_a values for the MC-N equilibria in 2-AP (protonation of pyridine =N–) [48] and 2-APBI [20] (protonation of benzimidazole =N–) are 6.86 and 3.42, respectively. In 2-A3PyBI, lone pair on the amino group is delocalized not only on the pyridyl ring but also on the BI moiety. Further the IHB between the amino group and BI =N– atom will be stronger in 2-A3PyBI as mentioned above than that in 2-APBI and thus makes the protonation of BI =N– atom more difficult in the former molecule. Thus pK_a values for the protonation of pyridine =N– and BI =N– will be less than those observed in the separate individual molecules. Our results are consistent with the above explanation i.e., 5.6 for protonation of pyridine =N– and 2.2 for the BI =N– atom. pK_a value for the protonation of –NH_2 group of the MC of 2-AP is −7.8 [48]. In the present case, even though the absorption spectrum has started blue shifting at H_0 = −10, indicating that protonation of –NH_2 group, but its formation is not complete in S_0 state. It is also supported by the decrease in the fluorescence intensity of the DC band (423 nm) without the appearance of any other new emission, agreeing with the fact that –NH_3^+ ion becomes stronger acid in S_1 state and thus requires stronger acidic medium than H_0 = −10 [50]. pK_a value for the deprotonation of >N–H group of BI in 2-APBI is 12.9 [20] whereas that of –NH_2 group in 2-AP is > 14. Thus smaller pK_a value (11.1) observed for the deprotonation of >N–H group of BI in 2-A3PyBI is due to the presence of electron withdrawing pyridine moiety. Lastly since the formation of DA is not complete at H_- = 15.9, its pK_a value will be greater than 14.8.

pK_a values of the respective prototropic equilibria in S_1 state (pK_a*) were determined by exciting at the respective isosbestic points and fluorimetric titration curves. In all cases the values obtained are the ground state values, suggesting

that prototropic equilibriums are not established in S_1 state. This is because of the shorter lifetimes of the respective conjugate acid–base pairs than the reciprocal rate constants of the protonation–deprotonation reactions.

6. Conclusions

Following conclusions can be made based on the above study. (i) Only one kind of DC and DA can be formed by protonating and deprotonating 2-A3PyBI. (ii) Trication starts forming in S_0 state but is unstable in S_1 state. (iii) Theoretical and experimental results confirm the formation of two kinds of MC in S_0 and S_1 states. MC2, formed by protonating pyridine =N– atom is more stable in polar solvents, leading to the large Stokes shifted emission due to tautomer, formed by ESIPT. MC3, formed by protonating BI =N– atom is stable in non-polar environments and gives rise to only small Stokes shifted normal emission. Equilibrium is not established in S_1 state, confirmed by two different lifetimes. (iv) MA is formed by deprotonating >N–H moiety of BI, leading to closed structure and large Stokes shifted emission belonging to tautomer anion, formed by ESIPT. SW small Stokes shifted emission can be assigned to open solvated structure. (v) This study also confirms that rate of ESIPT process can be increased by increasing the acidity of $–NH_2$ proton and basicity of the proton-accepting moiety.

Acknowledgements

Author is thankful to the Department of Science and Technology, New Delhi for the financial support to the project SP/S1/H-07/2000. The author is also thankful to Mr. M.M. Balamurali for carrying out the experimental work which forms part of his Ph.D. thesis.

References

[1] S.M. Ormson, R.G. Brown, Prog. React. Kinet. 19 (1994) 45.
[2] D. Legourrieve, S.M. Ormson, R.G. Brown, Prog. React. Kinet. 19 (1994) 211.
[3] M.C.R. Rodriguez, F. Rodriguez, M. Mosquera, Phys. Chem. Chem. Phys. 1 (1999) 253, and references listed there in.
[4] E.M. Kosower, D. Huppert, Ann. Rev. Phys. Chem. 37 (1986) 127.
[5] B.G. Malmstrom, Chem. Rev. 90 (1990) 1247.
[6] A.U. Khan, M. Kasha, Proc. Natl. Acad. Sci. U.S.A. 91 (1994) 8627.
[7] P.T. Chou, M.L. Martinej, Radiat. Phys. Chem. 41 (1993) 373.
[8] L.A. Hauch, C.L. Renschlae, Nucl. Instr. Math. A 235 (1985) 41.
[9] D.B. O'Connor, G.B. Scott, D.R. Coulter, A. Yavrouln, J. Phys. Chem. 95 (1991) 10252.
[10] T. Nishyiya, S. Yamuchi, N. Hirota, M. Baba, I. Hamazaki, J. Phys. Chem. 90 (1986) 5730.
[11] A. Syntnik, J. Carlos Devella, J. Phys. Chem. 99 (1995) 13208.
[12] S.K. Das, S.K. Dogra, J. Colloid Int. Sci. 205 (1998) 443, and references listed there in.
[13] G. Woolfer, P.J. Thistlethawite, J. Am. Chem. Soc. 103 (1981) 6916.
[14] J.F. Ireland, P.A.H. Wyatt, Adv. Phys. Org. Chem. 12 (1976) 643.
[15] T.P. Carter, M.M. Van Bentham, G.D. Gillispie, J. Phys. Chem. 87 (1998) 1891.
[16] T.P. Carter, G.D. Gillespie, M.A. Connolly, J. Phys. Chem. 86 (1982) 192.
[17] M.K. Nayak, S.K. Dogra, J. Photochem. Photobiol. A: Chem. 161 (2004) 169.
[18] M.K. Nayak, S.K. Dogra, J. Photochem. Photobiol. A: Chem. 169 (2005) 79.
[19] S. Scheiner, J. Phys. Chem. 104 (2000) 5998.
[20] A.K. Mishra, S.K. Dogra, J. Photochem. Photobiol. 31 (1985) 333.
[21] S. Santra, S.K. Dogra, Chem. Phys. 226 (1998) 285.
[22] T.P. Smith, K.A. Zaklika, K. Thakue, P.F. Barbara, J. Am. Chem. Soc. 113 (1991) 4035.
[23] S. Santra, G. Krishnamoorthy, S.K. Dogra, Chem. Phys. Lett. 311 (1999) 95.
[24] S. Santra, G. Krishnamoorthy, S.K. Dogra, J. Phys. Chem. A. 104 (2000) 476.
[25] S. Santra, G. Krishnamoorthy, S.K. Dogra, Chem. Phys. Lett. 327 (2000) 230.
[26] M.M. Balamurali, S.K. Dogra, Chem. Phys. 305 (2004) 147.
[27] R.W. Middleton, D.G. Wibberly, J. Heterocyclic. Chem. 17 (1980) 1757.
[28] G. Krishnamoorthy, S.K. Dogra, J. Org. Chem. 64 (1999) 6566.
[29] M.M. Balamurali, S.K. Dogra, J. Photochem. Photobiol. A: Chem. 154 (2002) 81.
[30] M.J. Jorgenson, D.R. Hartter, J. Am. Chem. Soc. 85 (1963) 878.
[31] Y. Yagil, J. Phys. Chem. 71 (1967) 1034.
[32] S.R. Meach, D.J. Phillips, J. Photochem. 23 (1983) 193.
[33] M.J.S. Dewar, E.G. Zeoblish, E.F. Healy, J.J. Stewart, J. Am. Chem. Soc. 107 (1985) 3902.
[34] H. Hinze, H.H. Jaffe, J. Am. Chem. Soc. 84 (1962) 540.
[35] J. Delbene, H.H. Jaffe, J. Chem. Phys. 48 (1989) 1807.
[36] N. Mataga, T. Kubata, Molecular Interactions and Electronic Spectra, Marcel Dekker, New York, 1970.
[37] E. Lippert, Z. Electrochem. 61 (1957) 962.
[38] M. Head-Gordon, E.S. Replogle, J.A. Pople, Gaussian 98, revision A. T Gaussian Inc. Pittsburg, PA, 1998.
[39] A.D. Becke, J. Chem. Phys. 98 (1993) 5648.
[40] R.G. Parr, W. Yang, Density-Functional Theory of Atoms and Molecules, Oxford University Press, New York, 1998.
[41] G.A. Peterson, M.A. Al-Lahan, J. Chem. Phys. 94 (1991) 6081.
[42] R. Bauernschmitt, R. Ahlrichs, Chem. Phys. Lett. 256 (1996) 454.
[43] M.E. Casida, G. Jamorski, K.C. Casida, D.R. Salahub, J. Chem. Phys. 105 (1998) 4439.
[44] H.K. Sinha, S.K. Dogra, Chem. Phys. 102 (1986) 337.
[45] P.B. Bist, H. Petek, K. Yoshihara, U. Nagashima, J. Chem. Phys. 90 (1995) 103.
[46] M. Krishnamurthy, S.K. Dogra, J. Photochem. 32 (1986) 235.
[47] P.C. Mishra, B.P. Asthana, QCPE No. 039, Quantum Chem. Program Exch. Bull. 9 (19873) 176.
[48] A. Weisstuch, A.C. Testa, J. Phys. Chem. 72 (1968) 1982.
[49] S.K. Das, S.K. Dogra, J. Chem. Soc. Perkin Trans. 2 (1999) 2771.
[50] M. Swaminathan, S.K. Dogra, J. Am. Chem. Soc. 105 (1983) 6223; A.K. Mishra, S.K. Dogra, Indian J. Chem. 24A (1985) 364; R. Manoharan, S.K. Dogra, Can. J. Chem. 65 (1988) 7013; R. Manoharan, S.K. Dogra, J. Phys. Chem. 92 (1988) 5282; R. Manoharan, S.K. Dogra, Bull. Chem. Soc. Jpn. 62 (1989) 1292; A. Paul, R.S. Sarpal, S.K. Dogra, J. Chem. Soc. Faraday Trans. I 86 (1990) 2095.
[51] A.K. Mishra, M. Swaminathan, S.K. Dogra, J. Photochem. 29 (1985) 87.